CEAS Space Journal
https://doi.org/10.1007/s12567-022-00455-y

ORIGINAL PAPER

Feasibility analysis of GNSS-based navigation for LUMIO mission

Franco Bernelli-Zazzera[1] · **Danilo Forte**[1]

Received: 20 February 2022 / Revised: 13 May 2022 / Accepted: 16 May 2022

Abstract
The paper presents the design of a realistic model of the GNSS constellations GPS and Galileo to perform a navigation performances analysis in lunar environment. Starting from the visibility analysis, the link-budget of each visible GNSS spacecraft is estimated using for each one realistic data for the transmitted power and environmental and system parameters. The navigation performances are evaluated in this scenario. The model implemented is applied to the trajectory of the LUMIO CubeSat mission and the results are commented. LUMIO is a lunar CubeSat mission, on a Halo orbit at the L2 point of the Earth–Moon system, designed to observe the measured meteoroid impacts on the far side of the Moon. LUMIO has been designed to perform autonomous onboard navigation with an accuracy better than 30 km for more than 99.7% of the time. The navigation analysis in this work can be compared to such a requirement to evaluate if a GNSS-based navigation solution could be employed as well.

Keywords GNSS · Lunar navigation · LUMIO mission

1 Introduction

Global Navigation Satellite Systems (GNSS) aim to provide navigation and timing services for users around the world, hence the name. Users flying in Medium Earth Orbit (MEO) or below are usually in an Earth-like configuration in terms of line-of-sight geometry and signal strength. From a functional point of view, the GNSS receiver of the spacecraft operating above MEO is like the ground receiver. If the signals of at least 4 satellites are received and processed, a navigation solution can be computed with accuracy depending on the pseudorange errors and geometric configuration. However, compared with the previous case, it faces three main challenges: low received signal strength, poor user/satellite geometry, and high Doppler shift and Doppler rate. To serve ground users, the antenna of each navigation satellite is pointed in the nadir direction. For users in the space above the MEO, except for some spillover, almost the entire main lobe is covered by the Earth. In most cases, only sidelobe's signals are received with a signal power for the GPS system about 15 dB lower [1, 2] with respect to main lobe ones. In addition, as the orbital height increases, the Free-Space Propagation/Path (FSP) loss becomes larger. At lunar altitude, these losses are 20 to 25 dB higher than low Earth orbit altitude. Due to the low received signal power and to ensure sufficient usability of the navigation solution, the GNSS receiver above the MEO should be designed to have higher tracking and acquisition sensitivity and should also be equipped with a high-gain antenna. Both will introduce more noise and errors in the navigation solution [3, 4]. The Geometric Dilution of Precision (GDOP), indicating how errors in the measurement will affect the final position estimation, also increases sharply as the height of the receiver increases, as the navigation satellites dwell in smaller and smaller field of view of the receiver. In addition to tracking most possible satellites, the GDOP is also limited due to the configuration of the GNSS constellation. For example, at the height of the Moon, the separation angle between the MEO satellite and the center of the Earth is less than 5°. Finally, as with all space based GNSS receivers, the predicted Doppler frequency shift and Doppler rate need to be estimated to obtain and continue to track the navigation satellite. In fact, the relative dynamics of velocity and acceleration are usually higher and more difficult to predict than ground users.

✉ Franco Bernelli-Zazzera
franco.bernelli@polimi.it

[1] Department of Aerospace Science and Technology, Politecnico di Milano, Milan, Italy

Published online: 29 June 2022

Conventional navigation in the lunar environment is performed on the ground using radiometry. Autonomous navigation can be very beneficial as a complementary, if not alternative, solution to traditional navigation methods, providing cost-effectiveness and simplifying operations. Even more so for smaller spacecraft, the development of such technological solutions is critical to extending the potential of nanosatellites beyond Earth orbit.

GNSS navigation in the lunar environment has not been tested but has been the subject of numerous model-based studies and analyses in recent years. Indeed, in the context of a growing interest in lunar exploration and commercial development, this technical solution is very interesting.

The highest altitude for operational GNSS receivers to obtain navigation solutions dates to 2017, being the on-board GPS receivers for Magnetosphere Multiscale Spacecraft (MMS) [5, 6]. The height of the apogee of the spacecraft's elliptical orbit is approximately 153,000 kms (40% of the Earth–Moon distance). The receiver has 12 channels, a tracking threshold of 22 db(Hz), and is equipped with an antenna with a peak gain of 7 dB. Experimental data showed promising results and higher than expected signal levels. A model-based analysis was developed in [6, 7] to evaluate GPS visibility and signal level, calibrated using data from the GOES-R and MMS receivers and applied to the Near-Rectilinear Halo Orbit (NRHO) that is the planned orbit for the Lunar Orbital Platform-Gateway. This indicates that if a 14 dB peak antenna is used, four or more Space Vehicles (SV) of the constellations can be seen in 67% of the trajectory.

The Galileo system as the second GNSS constellation has been discussed in [8], where it is estimated that a sensitivity of at least 20 db(Hz) is the minimum required to solve the navigation solution at lunar altitude. In [3, 9, 10], the design requirements for highly sensitive GNSS receivers are assessed, focusing on ESA's lunar lander, using GPS and the Galileo constellation. An acquisition and tracking strategy is proposed for the design of high sensitivity receivers and it is found that a threshold of 5 db(Hz) can be reached. With this tracking threshold and a receiving antenna with 10 dB peak gain, four SVs of the GPS or GALILEO constellation are always visible. Also, in [3], for a dual frequency receiver with a tracking threshold of 5 db(Hz), the error budget is calculated at 1.7 m and the main contributor to the error is the thermal noise of the receiver. The GDOP estimated at the height of the Moon is 400, which is equivalent to a PVT solution with an accuracy of <700 m.

The Lunar Gateway orbit is analysed in [11]. This article analyses the performance of a GNSS receiver capable of tracking all four GNSS (but still focusing on GPS + Galileo performance), with a tracking threshold of 15 db(Hz) and equipped with a peak gain antenna 14 dB, and its visibility analysis is performed. More than four SVs are still visible and tracked. Furthermore, the idea of evaluating the receiver's ability to autonomously demodulate navigation messages is presented in the form of ephemeris visibility, as opposed to tracking visibility. If the valid ephemeris data is demodulated from the navigation message within the prior 4 h, the satellite is considered visible. In such condition, the average SV visible during the simulation period is reduced by 2/3.

In this work, similar models and analyses are performed on the trajectory of the CubeSat Lunar Meteoroid Impact Observer (LUMIO). The LUMIO mission has completed the Phase A study [12], within which ESA has conducted an unpublished preliminary study on the suitability of GNSS navigation for the mission [13]. The objective of the present study is to systematise and extend the analysis of GNSS-based navigation for LUMIO, providing indications on its feasibility and under which conditions it can meet the requirements of navigation operations, evaluating the performance in its special halo orbit at the L2 point of the Earth–Moon system. The results obtained are promising: the navigation aspect is proven to be feasible, but with extremely challenging system engineering variables. Expecting advances in miniaturization of antennas and receivers, the GNSS navigation may soon become feasible also from a system engineering point of view.

2 The simulation models

2.1 GNSS constellations

The GNSS constellations simulated are GPS and Galileo, assuming their orbits as nominal and unperturbed and starting at their operational configuration at epoch 10 December 2020, 12:00 UTC. For each satellite, in addition to the pitch steering, a perfect yaw-steering attitude is assumed such that the transmit antenna points nadir towards Earth to service ground user and the solar panel axis stays normal to the Sun direction to maximize power generation. This imposes a continuous yaw rotation of the satellite around its nadir pointing antenna axis.

2.2 Receiver trajectory and performances

The user spacecraft and the on-board GNSS receiver are assumed to be a simple point body and thus are fully described at each epoch only by the state vector (position and velocity). No attitude is modelled nor included, since there is not a defined mission profile for the case analysed. The receiver front end in the model includes a High-Gain Antenna (HGA) and a Low Noise Amplifier (LNA). The HGA has 14 dBi peak gain at boresight and a 3 dB beamwidth of 12.2°. This antenna is the analogous to the one

defined in [11, 14]. but with a directivity assumed independent from the signal frequency and 0.75 antenna efficiency. The LNA has a gain of 30 dB and a noise figure of 2 dB. No receiver transmission loses are considered. An implementation loss of 2 dB, including A/D conversion is assumed. All those parameters are realistic and leaning toward a more conservative side. For the acquisition and tracking of the GNSS signal no loop is simulated. The receiver is assumed a "black box" and described only by its acquisition/tracking sensitivity in db(Hz).

The attitude of the spacecraft is not defined, it is assumed to be pointing the Earth center as a simple modelization. This is a strong assumption, for a small spacecraft without a gimbaled antenna which in general is the case for CubeSat. This is also an unlike assumption during manoeuvres. In normal operation though, the real antenna will obviously have a certain pointing error, but since the satellites are all in a field of view limited to $\pm 5°$ off-bore angle with respect to the Earth center at Moon altitude, corresponding to a 12 dB gain, under the hypothesis of ideal pointing we are in a range of at most 2 dB from that. In this sense the ideal pointing simulated would be comparable to the real pointing accounting for errors.

2.3 LUMIO trajectory

LUMIO is a lunar CubeSat mission designed to observe and measure the impact of meteoroids, that cannot be obtained from ground-based observations. The target orbit is a Halo at the L2 point of the Earth–Moon system, with a period of about half a synodic period. The mission has an expected mission lifetime of 1 year [15, 16], starting from the 21 March 2024 epoch to 21 March 2025. The trajectory is plotted in Fig. 1 and the orbit characteristics are listed in Table 1. In accordance with the mission requirements, LUMIO is designed to perform autonomous navigation on board. The baseline is an optical navigation system, that has been shown to meet navigation requirements with an accuracy of < 30 kms in more than 99.7% of the time [17]. The navigation analysis in this work can be compared with such requirements to evaluate the possibility to use GNSS-based navigation solutions as backup navigation system.

2.4 Link-budget estimation

The GNSS satellites are considered available if the line-of-sight between the receiver and the transmitting SVs is unobstructed neither by the Earth nor by the Moon and if the received signal power is above the receiver acquisition/tracking threshold. To evaluate the received signal power, the carrier to noise spectral density (C/N_0) is estimated at each epoch for each in line-of-sight, as

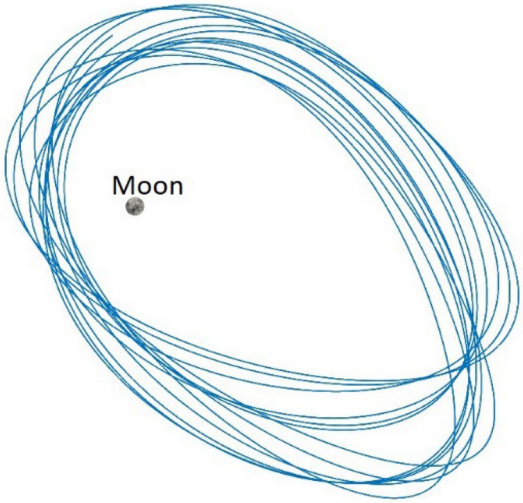

Fig. 1 LUMIO halo orbit

Table 1 LUMIO orbit characteristics

Min. Moon distance	35,078 km
Max. Moon distance	86,465 km
Halo period	14.74 days

$$C/N_0 = (C)_{dB} - \left(N_0\right)_{dB}[dB - Hz] \tag{1}$$

where $(C)_{\mathrm{dB}}$ is the received signal power in dB and $(N_0)_{\mathrm{dB}}$ is the thermal noise power in dB in a 1 Hz bandwidth. It is assumed that 0 dB = 10*$\log_{10}$(1 [W]) and this can be further detailed as

$$(C)_{dB} = \left(P_{Tx}\right)_{dB} + \left(G_{Tx}\right)_{dB} + \left(G_{Rx}\right)_{dB} - \left(A_d\right)_{dB} - L_{dB}[dBW] \tag{2}$$

$$\left(N_0\right)_{dB} = 10\log_{10}\left(k_b\left(T_{ant} + T_{amp}\right)\right)[dBW] \tag{3}$$

where [2, 4, 18, 19]:

$(P_{Tx})_{dB}$ is the signal transmitted power [dBW], $(G_{Tx})_{dBi}$ is the SV's antenna gain toward the receiver [dBi], $(G_{Rx})_{dBi}$ is the receiver's antenna gain toward the SV [dBi], $(A_d)_{dB}$ is the free-space propagation loss in dB [dB], L_{dB} is the receiver implementation loss, including A/D converter loss [dB], k_b is the Boltzmann's constants = 1.3806°23 [J/K], T_{ant} is the antenna noise temperature [K], T_{amp} is the amplifier noise temperature [K].

$(P_{Tx})_{dB}$ is the SV transmitted signal power in dBW. This value depends on the GNSS system considered, since it is function of the satellite design but also of the specific SV considered. In [20] the L-band transmitting power of each GNSS SVs operational at the time have been accurately estimated trough experimental measurements. Their

results are summarized in Table 2 and used in the current simulation model, where for GPS Block III-A, for which a measurement was not available, the transmitted power of Block IIF has been assumed. The total L-band emitted power is split between the signals. The sharing assumed in the simulation model is the one adopted in [11], that is 25% for GPS L1 and Galileo E1, and 50% for GPS L5 and Galileo E5a. The GPS L1 signal power allocation is evaluated in [19] and the same value has been used for the Galileo E1, while the GPS L5 signal power allocation is described in [18] and the same value has been used for the Galileo E5a signal. The remaining 25% power is assumed allocated to the other frequency bands not considered in the present study, i.e., L2 band for GPS and E5b and E6 for Galileo.

The transmitted power is then computed as

$$\left(P_{Tx}\right)_{dB} = 10\log_{10}\left(Power\ sharing \times Transmitted\ power\right) \tag{4}$$

$(G_{Tx})_{dBi}$ is the gain of the GNSS satellite antenna panel toward the receiver. Two-dimensional (off-bore angle and azimuth) antenna pattern are available for GPS Block IIR, IIR-M and IIF, the first two from the ground-test antenna gain measurements performed by Lockheed Martin (the satellites manufacturer) and from experimental reconstruction of the latter [1, 2]. For GPS Block III-A and Galileo, the same pattern and body reference frame of a GPS Block IIF SV has been used as modeling assumption.

$(G_{Rx})_{dBi}$ is the gain of the receiver antenna toward the SV considered. The antenna pattern is assumed symmetric and azimuth independent as previously described.

$(A_d)_{dB}$ is the free-space propagation loss in dB, computed as

$$\left(A_d\right)_{dB} = 20\log_{10}\left(\frac{4\pi f d}{c}\right) \tag{5}$$

where f is the signal frequency, d is the Tx-Rx distance and c is the speed of light in vacuum.

L_{dB} is the receiver implementation loss, including A/D conversion. In the model it is fixed at the value 2 dB, typical for a high-quality receiver and A/D converter [4].

Table 2 Average L-band transmitted power [20]

GNSS constellation	Type	Transmitted power [W]
GPS	IIR	60
GPS	IIR-M	145
GPS	IIF	240
Galileo	IOV	135
Galileo	FOV	265

T_{ant} is the sum of two contributions, one deriving from the ohmic losses due to inefficiencies in the antenna itself and one function of the thermal noise captured by the antenna at the signal frequency from external environmental sources. The antenna noise temperature due to its inefficiency can be computed as

$$\left(T_{ant}\right)_1 = T_p\left(\frac{1}{e_{ant}} - 1\right) \tag{6}$$

where T_p is the physical temperature of the antenna and e_{ant} is the antenna efficiency. In the model, 290 K is the assumed antenna physical temperature and $e_{ant} = 0.75$ has been selected for the antenna as a typical conservative value.

The second contribution to the antenna noise temperature is the thermal noise picked by the antenna from all the surroundings and can be computed in simplified form as [21]

$$\left(T_{ant}\right)_2 = T_p\left(\frac{\Omega_{\oplus}\left(25\ \mathrm{T_{b\oplus}}\right) + \Omega_{\leftmoon}\mathrm{T_{b\leftmoon}} + \left(4\pi - \Omega_{\oplus} - \Omega_{\leftmoon}\right)\mathrm{T_b}}{4\pi}\right) \tag{7}$$

where $\Omega_{\oplus}$ and $\Omega_{\leftmoon}$ are the solid angles subtended by the Earth and the Moon, respectively, as seen from the receiver and $T_{\mathrm{b}\oplus}$, $T_{b\leftmoon}$, T_{b} are the brightness temperature of the Earth, the Moon and of the cosmic background. The noise introduced by the Sun is considered negligible. This is a very good approximation unless the Sun is very close to the Earth from the satellite's point of view. In general, this is a rare occurrence, at most one day a month, as LUMIO flies in formation with the Moon at the Lagrangian point. Even in that case, given the much greater distance, it would be a contribution comparable to that introduced by the Earth, which is already very small compared to the total noise of the background radiation.

T_{amp} is the amplifier noise temperature. In the amplification stage other thermal noise is introduced, function of the quality of its realization. This effective temperature can be computed as

$$T_{amp} = Tp\left(10^{Nf} - 1\right) \tag{8}$$

where Nf is the amplifier noise figure which has been assumed equal to 2 dB as a typical value for a good LNA, and T_p is the physical temperature of the amplifier that in the model has been assumed as 290 K.

2.5 Simulation framework

The data of the simulated GNSS constellations, receiver trajectories and also the ephemerides and constants of the Earth, the Moon and of the Sun are first evaluated at fixed time steps. All the following computation are performed for each satellite of the GNSS constellations and for each

time step of the simulation. First the occultation of the line-of-sight of the receiver with respect to the SV considered is checked for the Earth or the Moon, modeled as ellipsoids. For each timestep where the receiver is not occulted, the attitude is computed as well as the relative state (position and velocity) and the relative angles. The main outputs are:

- The Tx-to-Rx distance,
- The Tx-to-Rx radial velocity,
- The spherical coordinate of the position vector of the receiver in the SV body frame, equivalent to the antenna pattern off-bore and azimuth angles,
- The off-bore angle of the SV with respect to the Earth pointed HGA of the receiver.

These outputs are used for the link-budget computation. At each time step in which the SV is visible, the Carrier-to-Noise ratio is computed following the described link-budget modelization and selected signal band.

The C/N_0 is then compared to receiver sensitivity and if it is above the threshold, an acquisition/tracking flag for that SV at that timestep is set to 1, else is set to 0. The GDOP is than computed for each constellation individually and for GPS + Galileo.

The ephemerides visibility analysis, which is described in the following section, can be performed for the GPS and Galileo constellations, returning for each SV and each timestep an ephemeris visibility flag, 1 if the SV is tracked and if its ephemerides have been demodulated in the past 4 h, else is set to 0.

2.6 Ephemerides visibility analysis

To assess whether the receiver can demodulate the navigation message, the received signal must be above the demodulation threshold long enough to allow the receiver to read all pages of the message. As in [11], the worst case is considered, assuming that the entire message is read. The threshold defined in [22] was used for the demodulation threshold. If the satellite carrier-to-noise signal is above the threshold for a long enough time, the satellite's ephemeris is assumed to have been demodulated. The ephemeris are valid and sufficiently accurate up to 4 h after recipient demodulation of the message. The values used for the analysis of the visibility of the ephemeris are listed in Table 3 and are consistent with the literature [11].

Therefore, the SV is considered visible if the SV is in the line of sight of the receiver, the C/N_0 signal is greater than the capture/tracking threshold and the satellite ephemeris has been demodulated in the last 4 h.

Table 3 Demodulation threshold and duration for each considered signal and message

Signal	Message	Threshold (db(Hz))	Duration (s)	Data validity (h)
L1	GPS LNAV	26.5	48	4
L5	GPS CNAV	26.1	24	4
E1	Galileo I/NAV	27.7	30	4
E5a	Galileo F/NAV	20.7	50	4

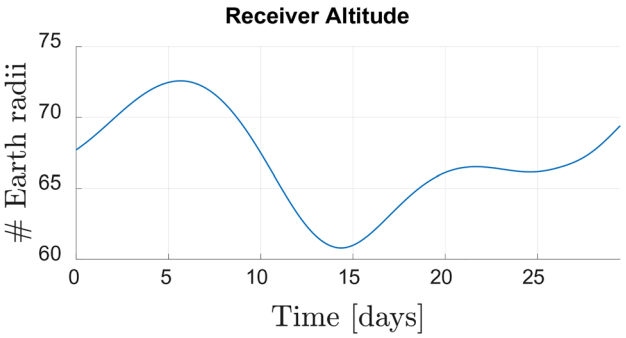

Fig. 2 LUMIO receiver altitude

2.7 LUMIO navigation performances

An Earth–Moon synodic period was simulated to evaluate navigation performance in two halo orbital periods. In Fig. 2, the temporal evolution of the altitude of the receiver is represented in Earth radii. Apart from small differences due to the cyclical variations (~every 18 years) of the orbital plane of the Moon and the secular motions, 1 month also covers the day in which the Earth–Moon distance is maximum.

The acquisition / monitoring threshold of 15 db(Hz) is used, the same as for the ESA IOD receiver [14] and, therefore, considered technologically feasible.

Figure 3 shows the availability of each SV during the simulation, i.e., if the satellite is in line of sight and if C/N_0 is above the acquisition / tracking threshold. The periodic occultations of the Earth for the GNSS satellites during their orbital motion are visible. Some SVs experience severe interruptions for a few days. These events are due to the relative geometry of the GNSS orbital plane and the lunar orbit and are independent from the trajectory of the receiver. Galileo visibility appears more regular, because it has only 3 and more stable orbital planes.

Figure 4 shows the total number of SVs available during the simulation. Almost always at least 4 satellites are visible. No lunar occultation occurs, due to the characteristics of LUMIO's orbit. Figure 5 shows the evolution of GDOP

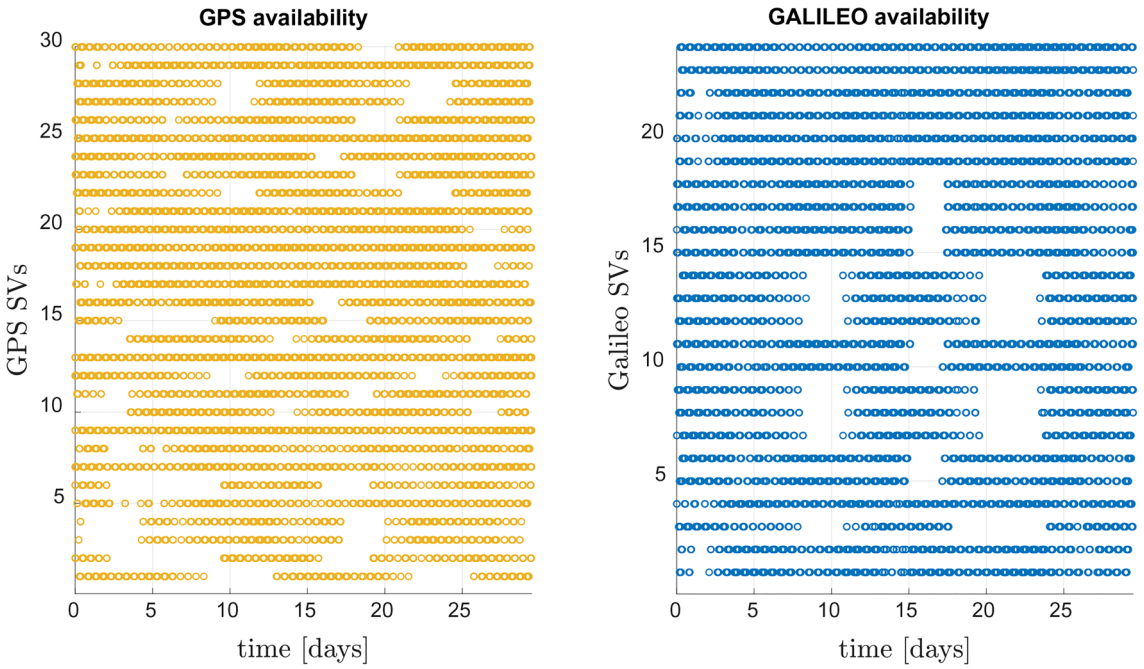

Fig. 3 Availability of each SV with time (15 db(Hz) threshold, L1/E1)

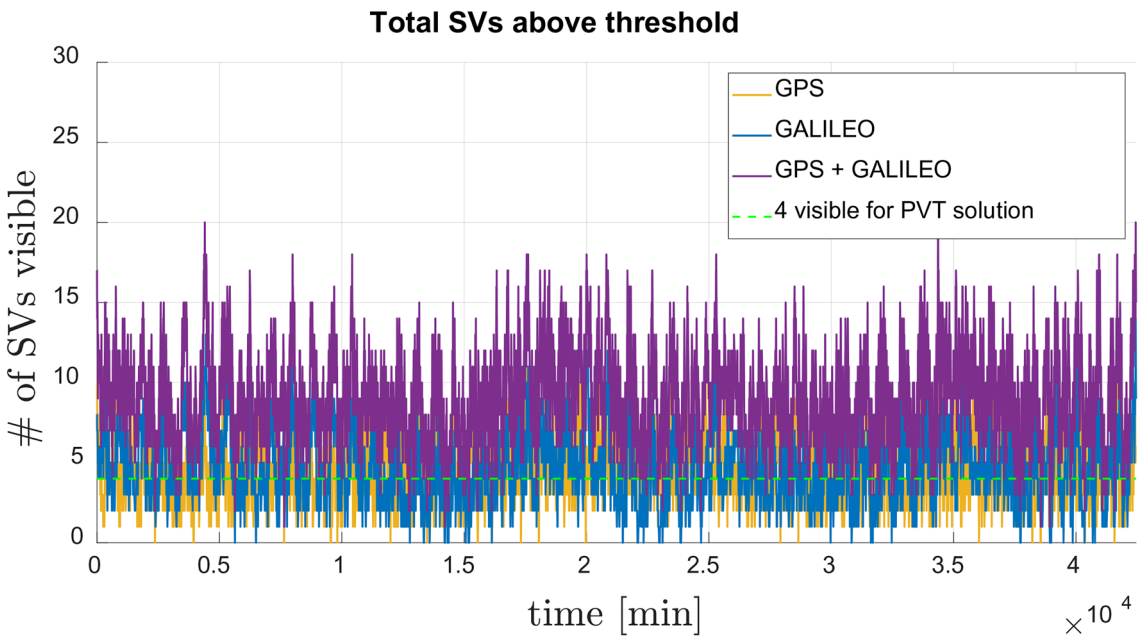

Fig. 4 Number of available SV with time (15 db(Hz) threshold, L1/E1)

during the simulation time. When using GPS + Galileo, the GDOP value is in the 10^3 range, but the value is quite unstable and shows large fluctuations.

In Figs. 6, 7 and 8 the same graphs are shown but for an L5/E5a receiver, including only the GPS IIF, III-A and Galileo SV blocks. Periodic interruptions in the visibility of specific SVs are greatly reduced due to the increase in received power and the beam width of this signal band. This results in more satellites available overall and, therefore, in a lower and more stable GDOP. The results are summarized in Table 4.

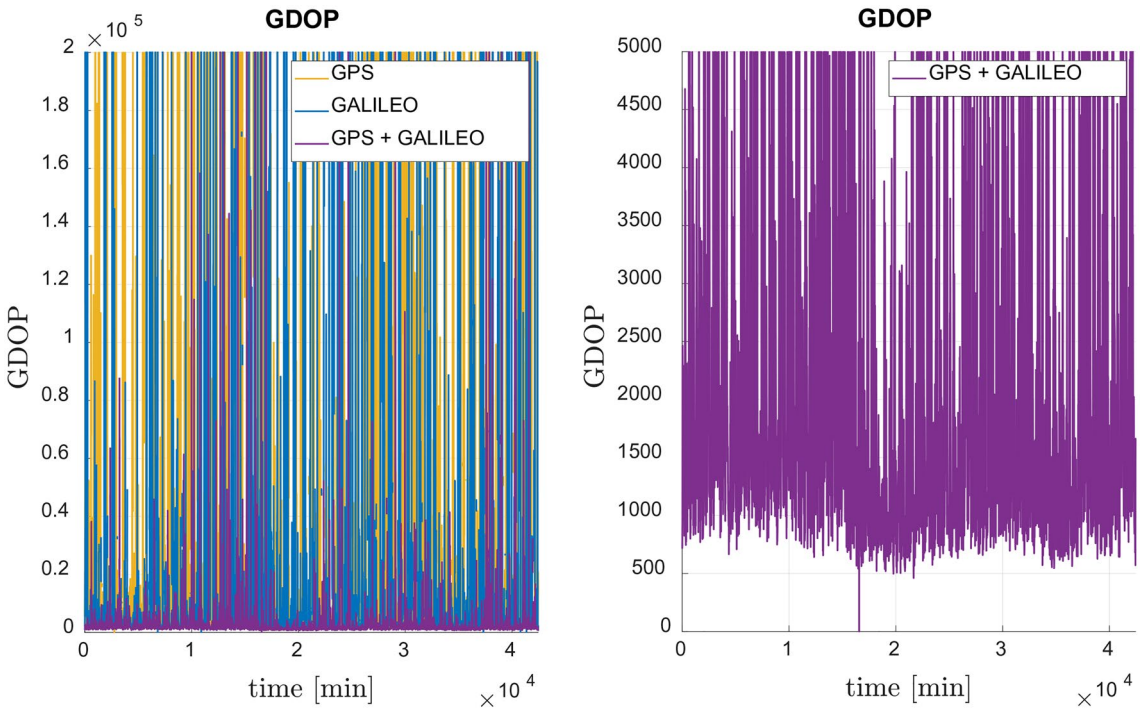

Fig. 5 GDOP evolution with time (15 db(Hz) threshold, L1/E1)

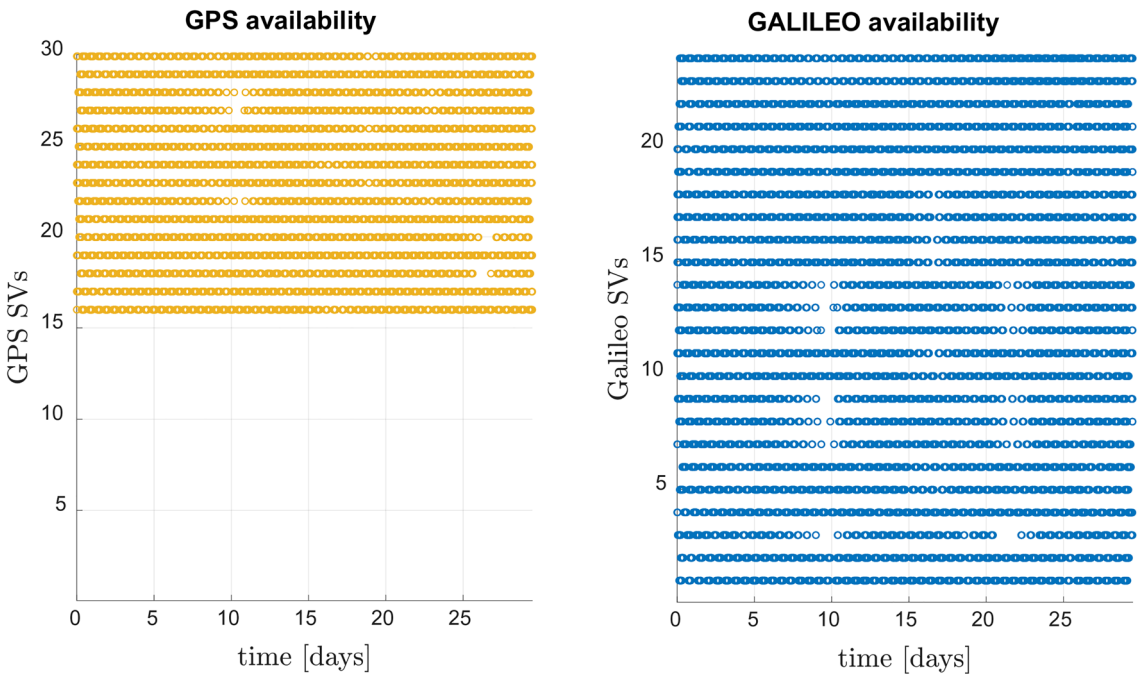

Fig. 6 Availability of each SV with time (15 db(Hz) threshold, L5/E5a)

The user error (UERE) is estimated following the same procedure as in [3], but assuming $\sigma_{te} = 7.5/0.75$ m, respectively, for the L1/E1 and L5/E5a receivers, to consider the higher orbital altitude of LUMIO of about 450,000 km:

$$UERE = \sqrt{\sigma_{ce}^2 + \sigma_{ee}^2 + \sigma_{me}^2 + \sigma_{re}^2 + \sigma_{te}^2} \tag{9}$$

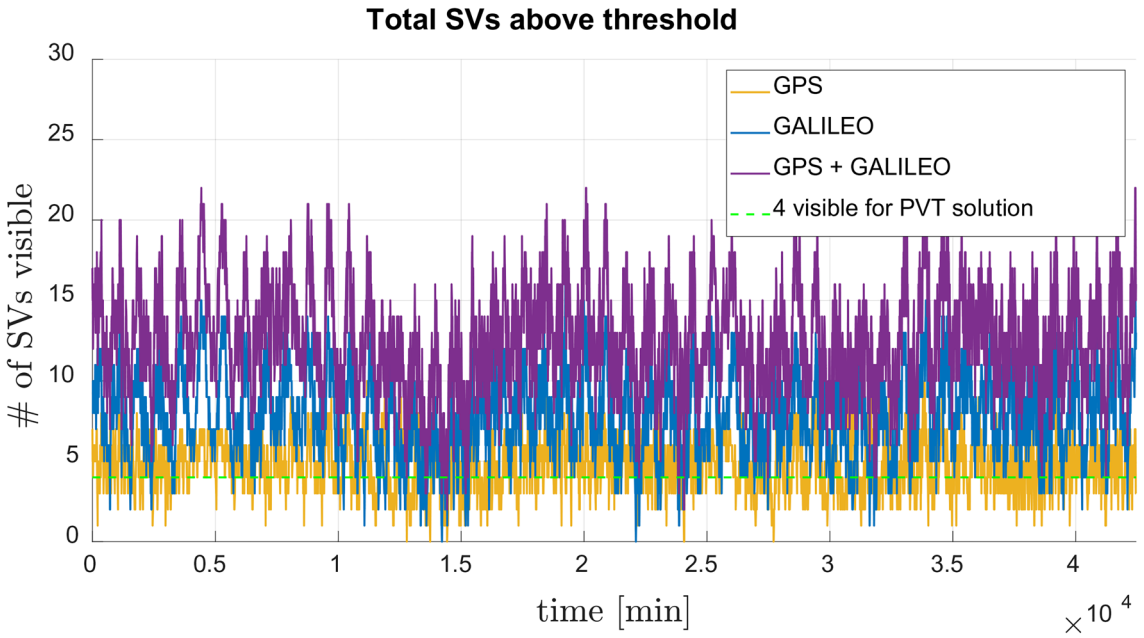

Fig. 7 Number of available SV with time (15 db(Hz) threshold, L5/E5a)

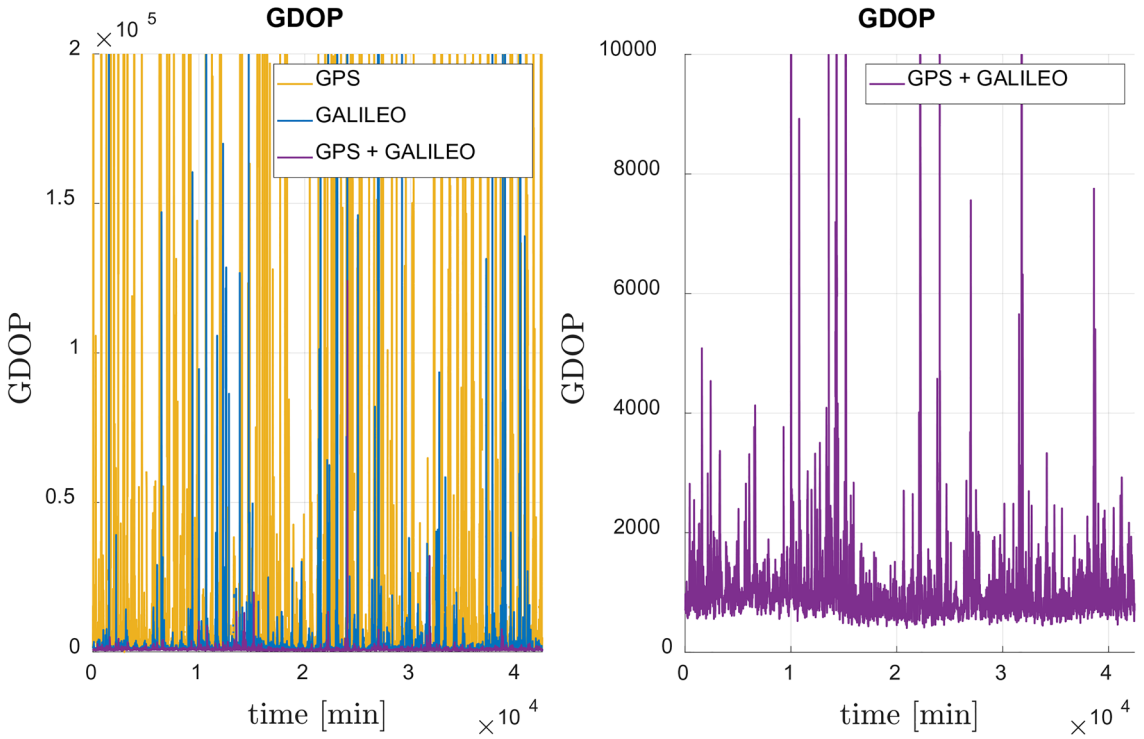

Fig. 8 GDOP evolution with time (15 db(Hz) threshold, L5/E5a)

Table 4 Navigation performances of the GNSS receiver on-board LUMIO

Signal	%≥4	# SVs available	Mean GDOP	UERE (m)	PVT accuracy (km)
L1/E1	98.8	9.02	3719.3	7.626	28.36
L5/E5a	99.9	12.6	980.3	1.569	1.538

where σ_{ce} is the broadcast clock error assumed equal to 0.8 m, σ_{ee} is the broadcast ephemeris range error assumed equal to 1.1 m, σ_{me} is the multipath error assumed equal to 0.2 m, σ_{re} is the receiver noise and resolution error assumed equal to 0.1 m and σ_{te} is the thermal noise code tracking error jitter function of the spacecraft altitude, of the acquisition/tracking threshold and of the chip-rate of the signal considered. The values assumed at Moon altitude for σ_{te} are tabulated in Table 5.

The navigation performances of the GPS + Galileo L5/E5a receiver are promising. Thanks to the lack of Moon occultations, 4 SVs are visible 99.9% of the simulated time and the position accuracy is lower than the ones of the LUMIO mission requirements. To evaluate if such a solution could be fully autonomous, the ephemerides analysis is needed.

An ephemeris visibility analysis was performed for both signal bands for the same simulation time of an Earth–Moon synodic period. The results are summarized in Table 6 and the availability of SV is shown in Fig. 9, where the visibility of the tracking is compared to the visibility of the ephemeris in the two signal bands. The same comparison is shown in Fig. 10 for the GDOP. Since this is aimed at being a standalone navigation, the receiver must demodulate the satellite ephemeris from the navigation message, thus the performance of the GPS + Galileo L1/E1 receiver is certainly insufficient to meet the navigation needs, given the estimated position accuracy of 1σ of approximately 950 km.

The performance of the GPS + Galileo L5/E5a receiver, on the other hand, is well below LUMIO's navigation requirements, with a navigation solution available 99.5% of the time and with a position accuracy of $1\sigma < 3$ km. As the results are an order of magnitude below the requirements, the simulation confirms the feasibility of using a GNSS-based autonomous navigation solution for the LUMIO mission, assuming a sensitivity of at least 15 db(Hz) and a high-gain antenna.

Table 5 σ_{te} at Moon altitude for the thresholds and the signal band considered

Signal	15 db(Hz)	10 db(Hz)	5 db(Hz)
L1/E1	5 m	7.5 m	10 m
L5/E5a	0.5 m	0.75 m	1 m

Table 6 LUMIO trajectory tracking and ephemerides visibility and navigation performances

Visibility	Signal	%≥4	# SVs available	Mean GDOP	PVT accuracy (km)
Tracking	L1/E1	98.8	9.02	3719.3	28.36
	L5/E5a	99.9	12.6	980.3	1.538
Ephemerides	L1/E1	31.0	2.72	124,706	951.0
	L5/E5a	99.5	10.3	1757.6	2.757

2.8 Comparison with ESA study

ESA has conducted a Phase A study on the suitability of GNSS navigation for the LUMIO mission [13]. The study assumes a tracking threshold of 15 db(Hz) and an Earth-pointing antenna of 14 dB for the front end of the receiver. The feasibility of this solution is also demonstrated and an L5/E5a receiver is suggested as the preferred design choice, consistent with the results of the present study. The ESA study estimates an average availability of 11 SV, whereas in the present study this number is higher than 12. The lower value in the ESA study is probably due to the use of the real antenna model for Galileo, not publicly available.

Figure 11 shows the estimated number of available satellites in the ESA study for an L5/E5a receiver. This figure can be directly compared (apart from a different colour scheme) with Fig. 7. The results are quite similar, except for a slightly different availability. The estimated PDOP (GDOP analogue) is shown in Fig. 12. This figure can be compared with Fig. 8. The graphs are quite similar and, in both cases, an average GDOP of around 1000 is estimated, further validating the results presented in this study.

3 Conclusions

The results of this work demonstrate the feasibility of GNSS-based navigation in the lunar environment, complementing the literature on the subject. The model, calibrated based on the established results, was applied to future planned ESA lunar missions, such as LUMIO. Excellent performance was simulated, and an estimated 2-to-3-km position accuracy was demonstrated.

The usefulness of autonomous GNSS-based navigation for the LUMIO mission was demonstrated by proposing a single-frequency GPS + Galileo L5/E5a receiver, with a sensitivity of 15 db(Hz), a solution with an estimated

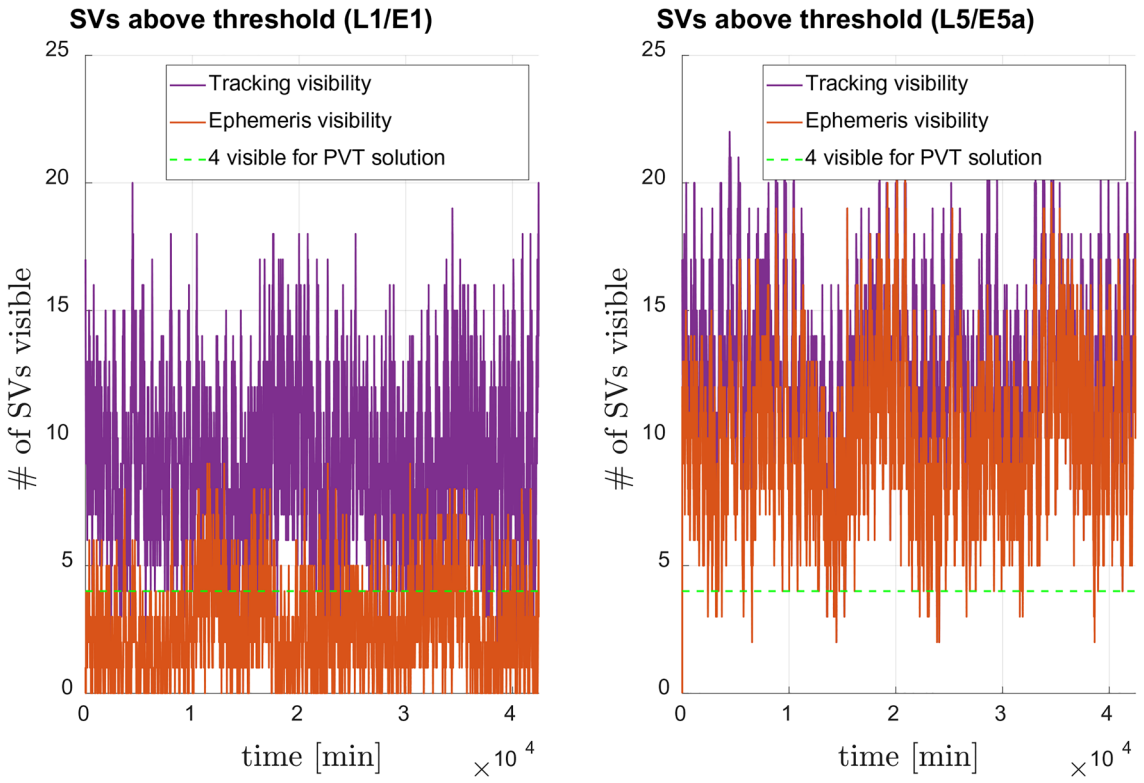

Fig. 9 Available SVs, tracking and ephemeris visibility comparison (15 db(Hz) threshold)

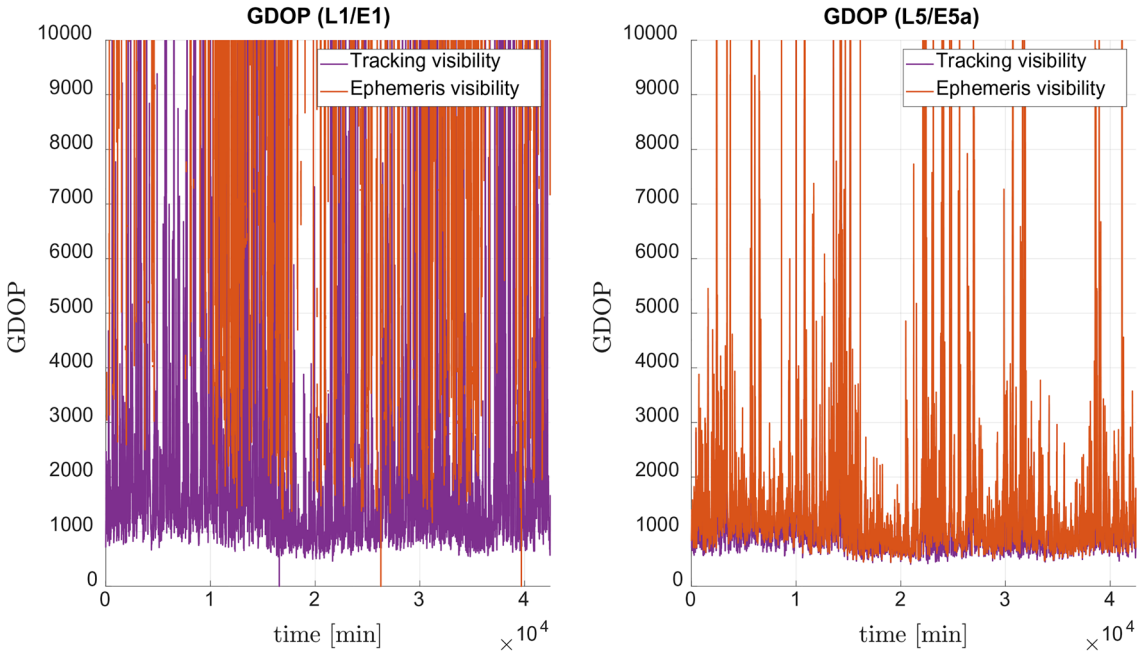

Fig. 10 GDOP, tracking and ephemeris visibility comparison (15 db(Hz) threshold)

technological readiness level (TRL) of about 6/7. Thus, the navigation solution has been proven to be feasible. However, preliminary considerations on the comparison with the baseline optical navigation solution indicate that further improvements and research are still needed, especially as regards its application to small spacecraft. In-orbit

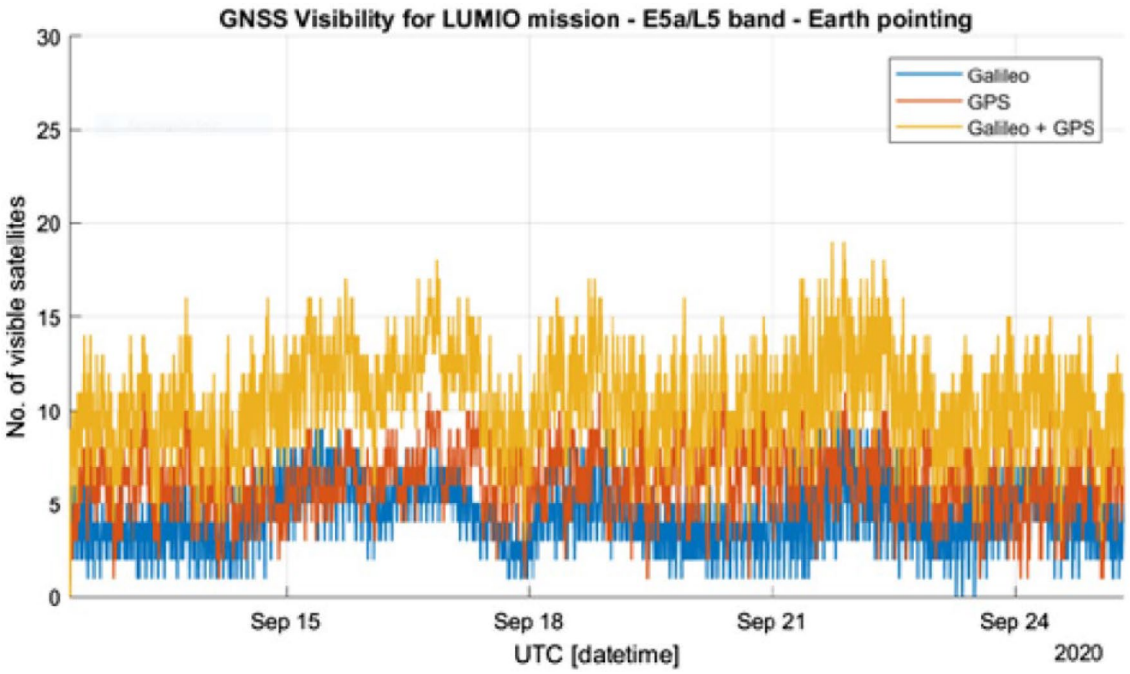

Fig. 11 Available SVs with time (L5/E5a band, ESA Phase A study [13])

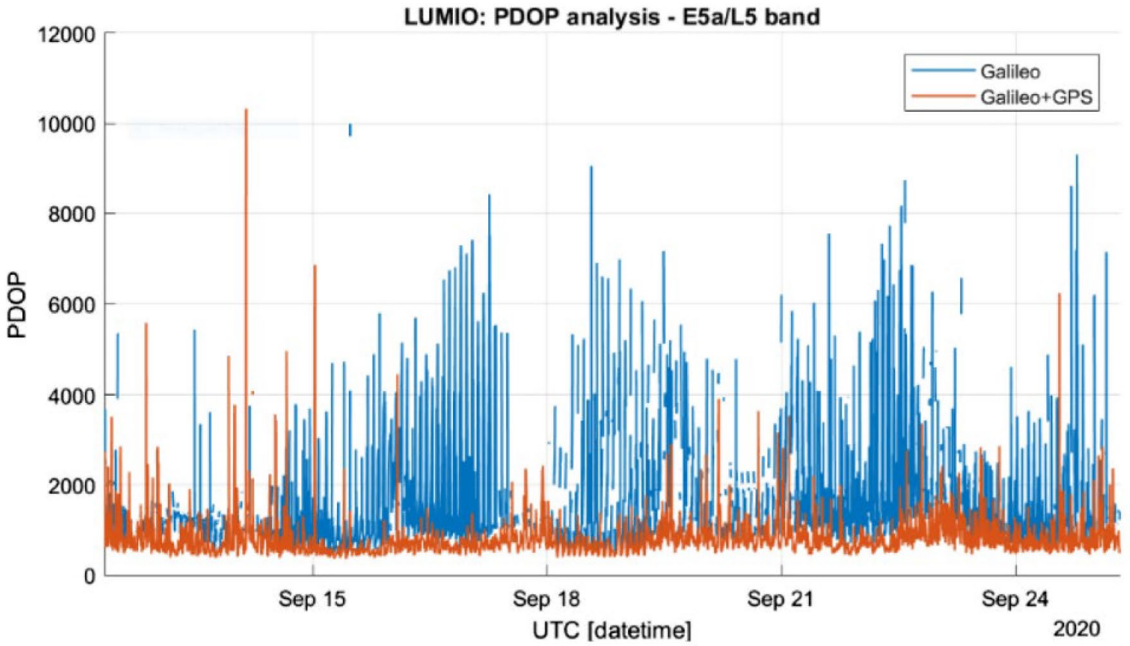

Fig. 12 Estimated PDOP (L5/E5a band, ESA Phase A study [13])

demonstration is needed both for the final demonstration of the technology and for improving the models using real experimental data. The first use of the GNSS receiver in lunar orbit is expected in the next 2 years, with the Lunar Pathfinder mission scheduled for launch by ESA in 2023, that will carry an experimental GNSS receiver.

In addition, estimation of the preliminary dimensions and mass of the antenna for LUMIO are described in [14] and are in the order of $260 \times 260 \times 175$ mm^3 and 2 kg. The antenna

data comes from ESA's statement of work for the Lunar Pathfinder receiver design. Note that Lunar Pathfinder is not a CubeSat so it is certainly possible that a more efficient solution with deployable antenna could be possible. In any case, for CubeSat 12U with a maximum mass of 22 kg, as for the LUMIO mission, such an antenna would use a considerable portion of the mass budget even without considering the GNSS receiver itself. For this reason, even if a GNSS-based solution could meet the requirements from a navigation performance point of view, this implementation is not considered appropriate for the mission. Furthermore, it lacks the elegance and simplicity of autonomous optical navigation based solely on the optical camera, which is already the main payload of the mission. It is remarked that the limiting factor is the navigation message demodulation threshold, for which a large antenna is required to use GNSS signal from the sidelobes. So long as the receiver must recover the ephemerides from the navigation message, there is no turnaround from this requirement. If the ephemerides are instead computed on-board using a long-term orbital and clock models, a smaller antenna could be used, and the performances improved by reducing the receiver acquisition/tracking threshold.

Hopefully, exploiting future advances in miniaturization of antennas and receivers, the GNSS navigation may become appealing also from a system engineering point of view, even for smaller spacecraft.

It is highlighted that the present results can be useful for the implementation of GNSS navigation in the entire cislunar space. The analysis, performed for one specific mission, covers distances from Earth in the range from 380,000 to 460,000 km and for the case in which Moon occultation of GNSS signals is not relevant. As such, any other mission planned in this range would be in the same conditions presented here and could exploit GNSS navigation with the same navigation performances foreseen for the LUMIO case.

Funding Open access funding provided by Politecnico di Milano within the CRUI-CARE Agreement. No funds, grants, or other support was received.

References

1. Donaldson, J.E., et al.: Characterization of On-Orbit GPS transmit antenna patterns for space users. Navigation (2020). https://doi.org/10.1002/navi.361
2. Marquis, W.A., Reigh, D.L.: The GPS block IIR and IIR-M broadcast L-Band antenna panel: its pattern and performance. Navigation (2015). https://doi.org/10.1002/navi.123
3. Capuano, V., et al.: Feasibility study of GNSS as navigation system to reach the Moon. Acta Astronaut. (2015). https://doi.org/10.1016/j.actaastro.2015.06.007
4. Kaplan, E.D., Hegarty, C.J.: Understanding GPS: principles and applications. Artech House (2006)
5. Ashman, B.W., et al.: GPS operations in high earth orbit: recent experiences and future opportunities. AIAA SpaceOps Conference (2018). https://doi.org/10.2514/6.2018-2568
6. Winternitz, L.B., Bamford, W.A., Price, S.R.: New high-altitude gps navigation results from the magnetospheric multiscale spacecraft and simulations at lunar distances. ION GNSS+ (2017). https://doi.org/10.33012/2017.15367
7. Ashman, B.W. et al.: Exploring the limits of high altitude gps for future lunar missions. Annual AAS Guidance & Control Conference (2018)
8. Palmerini, G.B., Sabatini, M., Perrotta, G.: En route to the Moon using GNSS signals. Acta Astronaut. (2009). https://doi.org/10.1016/j.actaastro.2008.07.022
9. Manzano-Jurado, M. et al.: Use of weak GNSS signals in a mission to the moon. 7th ESA Workshop on Satellite Navigation Technologies and European Workshop on GNSS Signals and Signal Processing (NAVITEC) (2014). https://doi.org/10.1109/NAVITEC.2014.7045151
10. Musumeci, L., et al.: Design of a high sensitivity GNSS receiver for lunar missions. Adv. Space Res. (2016). https://doi.org/10.1016/j.asr.2016.03.020
11. Delépaut, A., et al.: Use of GNSS for lunar missions and plans for lunar in-orbit development. Adv. Space Res. (2020). https://doi.org/10.1016/j.asr.2020.05.018
12. Cervone, A: et al.: Phase A Design of the LUMIO Spacecraft: a CubeSat for Observing and Characterizing Micro-Meteoroid Impacts on the Lunar Far Side. In: 71st International Astronautical Congress, (2020)
13. Delépaut, A.,Giordano, P.: LUMIO Phase A – GNSS Receiver Opportunities (2020)
14. ESA. Earth Moon GNSS spaceborne receiver for In-Orbit Demonstrations. NAVISP-EL1-039, (2020)
15. Dei Tos, D.A., Topputo, F.: Trajectory refinement of three-body orbits in the real solar system model. Adv. Space Res. (2017). https://doi.org/10.1016/j.asr.2017.01.039
16. Dei Tos, D.A., Topputo, F.: On the advantages of exploiting the hierarchical structure of astrodynamical models. Acta Astronaut. (2017). https://doi.org/10.1016/j.actaastro.2017.02.025
17. Franzese, V., Di Lizia, P., Topputo, F.: Autonomous optical navigation for the lunar meteoroid impacts observer. J. Guidance Control Dyn. **10**(2514/1), G003999 (2019)
18. Kwan, P.: IS-GPS-705F NAVSTAR GPS Space Segment/User Segment L5 Interfaces. GPS Directorate - Space & Missile Systems Center (SMC) - LAAFB (2019). https://navcen.uscg.gov/pdf/gps/IS_GPS_705F.pdf
19. Li, W., et al.: The Impact of inter-modulation components on interferometric GNSS-reflectometry. Remote Sensing (2016). https://doi.org/10.3390/rs8121013
20. Steigenberger, P., Thoelert, S., Montenbruck, O.: GNSS satellite transmit power and its impact on orbit determination. J. Geodesy (2018). https://doi.org/10.1007/s00190-017-1082-2

21. International Telecommunication Union. Radio noise. Recommendation ITU-R P.372-14 (2019). https://www.itu.int/dms_pubrec/itu-r/rec/p/R-REC-P.372-14-201908-S!!PDF-E.pdf
22. Anghileri, M., Paonni, M., Fontanella, D., Eissfeller, B.: GNSS data message performance: a new methodology for its understanding and ideas for its improvement. International Technical Meeting of The Institute of Navigation, pp 638–650 (2013). https://www.ion.org/publications/abstract.cfm?articleID=10839